Article

Novel High-Pressure Nanocomposites for Cathode Materials in Sodium Batteries

Aleksander Szpakiewicz-Szatan[1,2], Szymon Starzonek[2,*], Tomasz K. Pietrzak[1], Jerzy E. Garbarczyk[1,*], Sylwester J. Rzoska[2] and Michał Bućkowski[2]

[1] Faculty of Physics, Warsaw University of Technology, Warsaw, Poland
[2] Institute of High Pressure Physics of the Polish Academy of Sciences, Warsaw, Poland
* Correspondence: starzoneks@unipress.waw.pl (S. S.), jerzy.garbarczyk@pw.edu.pl (J. E. G.)

Abstract: New nanocomposite material was prepared by high pressure processing of starting glass of nominal composition $NaFePO_4$. Thermal, structural, electrical and dielectric properties of the prepared samples were studied by differential thermal analysis (DTA), X-ray diffraction (XRD) and broadband dielectric spectroscopy (BDS). It was demonstrated that high pressure – high temperature treatment (HPHT) led to an increase of electrical conductivity of initial glasses by 2 orders of magnitude. It was also shown that the observed effect was stronger than for lithium analogue of this material studied by us earlier. The observed enhancement of conductivity was explained by Mott's theory of electron hopping, which is more frequent in sample after pressure treatment. The final composite consisted of nanocrystalline NASICON and alluaudite phases, which are electrochemically active in potential cathode materials for Na batteries. Average dimensions of crystallites estimated from XRD studies were between 40 and 90 nm, depending on the phase. Some new aspects of local dielectric relaxations in studied materials were also discussed. It was shown that a combination of high pressures and BDS method is a powerful method to study relaxation processes and molecular movements in solids. It was also pointed out that high-pressure cathode materials may exhibit higher volumetric capacities compared with commercially used cathodes with carbon additions.

Keywords: high pressures; nanocomposites; cathode materials; conductive glasses; hopping conductivity; Na-Ion batteries

1. Introduction

Development of novel functional materials plays a significant role in emerging better and better technologies that have a significant impact on our every-day lives. In particular, green transformation of transport systems and power plants (from fossil fuels to zero emission), as well as faster development of portable electronics urge for better green energy sources, including portable batteries, stationary energy magazines and fuel cells. Currently, the battery market is dominated by Li-ion cells, which are used in a wide variety of products, spreading from small portable electronics to electric vehicles and trucks. On the one hand, limited abundance of lithium is one of the limiting factors for further development of Li-ion technologies and cathodes manufacturing costs are the most important part of the total battery costs. On the other hand, large stationary energy storage facilities need to be built as essential parts of renewable power plants (solar or wind) whose energy production is very dependent on the weather conditions. Hence, interest in sodium superionic conductors has recently revived.

Mixed electronic-ionic (Na^+) phosphate conductors are among intensively studied candidates for Na-ion batteries. These include NASICON-type materials (e.g. $Na_3M_2(PO_4)_3$ [1] or $Na_3M_2(PO_4)_2F_3$ [2,3], where M – transition metal ion, e.g. Fe, V, Mn, Ti) or alluaudites (e.g. $Na_xM_3(PO_4)_3$ [4,5]). $NaFePO_4$ is a sodium analogue of $LiFePO_4$ olivine, proposed in 1997 by J.B. Goodenough[6]. It shares its lithium counterpart features, such as relatively high gravimetric capacity (154 mAh/g), abundant composition, low manufacturing costs,

 doi:10.20944/preprints202212.0267.v1

low impact on the environment [7]. The olivine phase of NaFePO4 is unstable at ambient conditions. The stable phase of NaFePO4 is Maricite (space group Pmnb), whose electrochemical performance was modest (e.g. [8]). However, it was discovered that $NaFePO_4$ in amorphous form can exhibit much better performance, i.e. 142 mAh/g [9,10].

Usually, phosphate cathode materials exhibit modest electrical conductivity that may be a limiting factor for their performance in electrochemical cells. The most popular way of overcoming the limited conductivity is the addition of carbon during material syntheses or cathode preparation. The drawback of this approach is a decrease in the volumetric electrochemical capacity of such cathodes. Thermal nanocrystallization of glassy analogues of cathode materials may be an alternative way to significantly increase electrical conductivity of cathode materials [11]. This approach consists of two steps: i) a synthesis of glassy precursor; ii) its proper heat-treatment to induce appearance of nanocrystalline grains in a residual glassy matrix. The microstructure of such nanocrystalline materials provides favorable conditions for electronic hopping between aliovalent ions (e.g. Fe^{2+}/Fe^{3+} or V^{4+}/V^{5+}). Application of this technique led to a giant increase in the conductivity in numerous phosphate glasses, including $LiFe_{1-2.5x}V_xPO_4$ (i.e. $LiFePO_4$ with partial substitution of Fe^{2+} with V^{5+}), where nanocomposite materials with conductivity as high as ca 10 mS/cm at room temperature were obtained [12]. This phenomenon was qualitatively explained on the basis of Mott's theory of polaron hopping [13,14]. It was also shown that the same approach led to noticeable increase in the conductivity of sodium mixed conductors, i.e. NASICON-type [15] and alluaudite-type [16,17]].

In case of LiFePO4, it was also experimentally proved that application of high pressure (of order of GPa) has a significant influence on electronic conductivity [18]. In compressed nanomaterials, the distances between the hopping centers are smaller than in pristine glasses and hence irreversible increase of the electronic conductivity. In this work, we applied this approach to a sodium analogue of olivine, i.e. amorphous $NaFePO_4$ doped or undoped with vanadium. The purpose of this work was to investigate the influence of high pressure and high temperature treatment (HPHT) on electrical conductivity of this candidate for cathode in sodium-ion batteries.

2. Experimental

2.1. Preparation of glasses

Our initial aim was to prepare a glassy analogue of sodium olivine of nominal composition $NaFePO_4$. Being aware that preparation of pure glass of such composition may be difficult we have added some amount of V_2O_5 to selected samples as a supporting glass former. The nominal composition of such heterogeneously doped glasses was $NaFe_{0.85}V_{0.10}PO_4$.

To prepare the glasses, a melt quenching method, described by us elsewhere [18], was used. Appropriate amounts of: Na_2CO_3, $FeC_2O_4{\cdot}2H_2O$, $NH_4H_2PO_4$ and V_2O_5, were mixed in stoichiometric quantities and then finely ground in a planetary zirconia ball mill. Next the substrates were put into a crucible, which was placed in a furnace. Samples were gradually heated up to 1523 K and then kept at this temperature to complete the calcination reaction related to release of volatile components. Finally, the molten glass was poured on the stainless steel or copper plate and immediately covered with a similar plate. It was noticed that quenching on copper was more effective because in such a case it was not necessary to dope $NaFePO_4$ with vanadium to obtain a glass. An additional drawback of glasses doped with vanadium was their larger fragility compared to undoped glasses.

2.2. Experimental methods

Differential thermal analysis (DTA) which allowed to determine glass transition (T_g) and crystallization (T_c) temperatures of studied glasses were conducted using the TA Instruments Q600 SDT with a heating rate of 10 K/min in the range from 323 K up to 1073 K in Ar flow.

 doi:10.20944/preprints202212.0267.v1

X-ray Diffraction (XRD) measurements was performed using Phillips X'PerT PRO with Cu K_α (λ = 1.54 Å) in the range of Bragg angles from 5 to 115°(narrowed to the range 10–80° during analysis). Data was analyzed with the PANalytical High Score Plus software.

Electrical properties were measured with Broadband Dielectric Spectroscopy (BDS) using Novocontrol Alpha-A High Performance Frequency Analyzer in the frequency range between 10 mHz and 1 GHz (narrowed to 100 mHz –10 MHz during analysis) in temperatures ranging from 123 K to 473 K. The results were analyzed with the use of the Novocontrol WinFIT software with use of the multiple Havriliak-Negami functions.

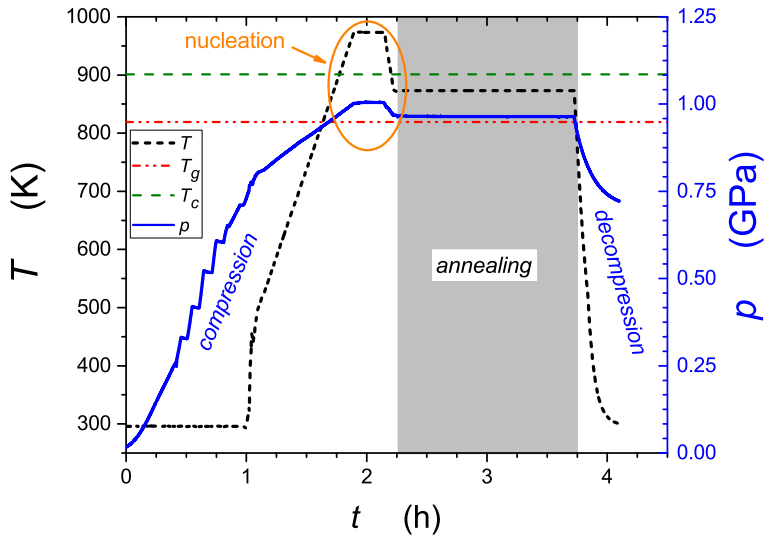

Figure 1. The course of high pressure-high temperature treatment (HPHT) used in this study. After 2 h of compression the annealing process started. Above crystallization temperature (T_c) the nucleation takes place.

The prepared NaFePO4 glasses were subjected to high pressure – high temperature treatment (HPHT), which was a key step in the present study. Developed in our lab HPHT method (1) is based on simultaneous action of isostatic high pressure (HP) and high temperature (HT). A sample of glass was put in the graphite crucible and then in a high-pressure chamber[19]. The chamber allowed to regulate the pressure of inert gas (N_2) and its temperature by use of a graphite resistor heater. Temperature measurements were carried out by means of system of thermocouples, which allowed to perform thermal analysis similar to DTA method (in this technique ΔT is defined as a difference between the temperature of the sample and the chamber).

In order to initiate nucleation of nanocrystallites, the glass sample was subjected to 1 GPa pressure, then heated up to 974 K (i.e. above T_c measured under pressure) and annealed at this temperature for 15 minutes. Next the sample was cooled down to 873 K (i.e. below T_c measured under pressure) and annealed for further 1,5 hour. Finally it was cooled down to room temperature while decompression to atmospheric pressure. Our long-time monitoring showed that the effect of HPHT on samples properties (conductivity) lasted for months.

Preprints (www.preprints.org) | NOT PEER-REVIEWED | Posted: 15 December 2022 doi:10.20944/preprints202212.0267.v1

3. Results

3.1. Differential Thermal Analysis

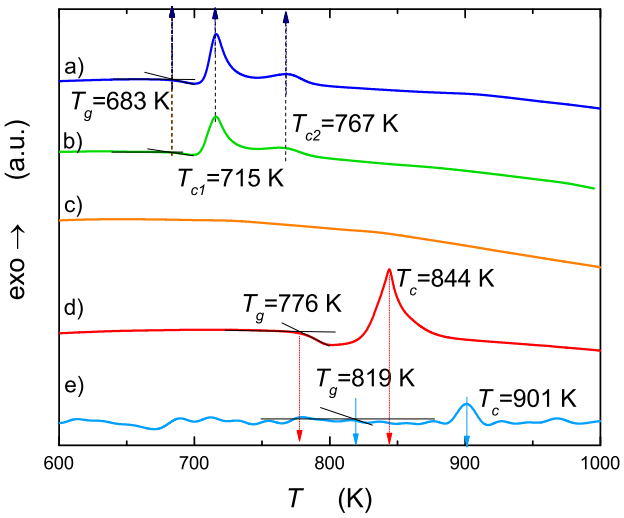

Figure 2. DTA runs of studied samples: a) $NaFe_{0.85}V_{0.10}PO_4$ glass quenched on a steel plate (NFV/st), b) $NaFe_{0.85}V_{0.10}PO_4$ glass quenched on a copper plate (NFV/co), c) $NaFePO_4$ quenched on steel (NF/st), d) $NaFePO_4$ glass quenched on copper (NF/co), e) $NaFePO_4$ glass quenched on copper (NF/co/HPHT), measured under pressure of 1 GPa.

Thermal analysis is a useful experimental technique because it gives information about the upper limit of thermal stability and phase transitions occurring in studied materials. Results of DTA are summarized in Figure 2 and Table 1.

Table 1. Glass transition (T_g) and crystallization (T_{c1}, T_{c2}) temperatures of studied samples

Sample	T_g [K]	T_{c1} [K]	T_{c1} [K]
a) NFV/st	683	715	767
b) NFV/co	683	715	767
c) NF/st	-	-	-
d) NF/co	776	844	-
e) NF/co/HPHT	819	901	-

Thermograms characteristic for glassy samples consist of endothermic shift corresponding to a glass transition and exothermic peak (or peaks) corresponding to crystallization of glass. For vanadium containing samples, a glass transition (T_g=683 K) and two crystallization peaks (T_{c1}=715 K, T_{c2}=767 K) are observed regardless of the cooling technique (steel or copper) used during melt quenching. For $NaFePO_4$ melt quenched between steel plates (st), no measurable glass transition nor crystallization peak has been observed that confirmed crystalline state of that sample. On the other hand a melt of the same composition quenched between copper plates (co) gives a glass with glass transition at about 776 K and only one crystallization peak at 844 K. It is worth noting at this point that: i) vanadium heterogeneous dopant helps to receive a glassy state in the case when steel plates are used (vanadium oxide plays a role of supporting glass former), ii) copper plate, due to its larger heat conductivity, is better and vanadium doping is not necessary in that case, iii) resignation from doping with vanadium and use of copper plates increases thermal stability of studied glasses from 683 to 776 K.

 doi:10.20944/preprints202212.0267.v1

Curve e in Figure 2 shows DTA run corresponding to NF/co glass subjected to a high pressure. In this case the values of T_g and T_c again increase approaching the values: 819 K and 901 K respectively that widens the supercooled range.

3.2. X-ray Ray Diffraction

X-ray diffractogram of the sample after high pressure/high temperature treatment contains many peaks coming from basically two crystalline phases (curve e in Figure 3). Comparing patterns c) and e) in Figure 3 one can notice appearance of new crystalline phases after HPHT treatment, not observed in pattern c.

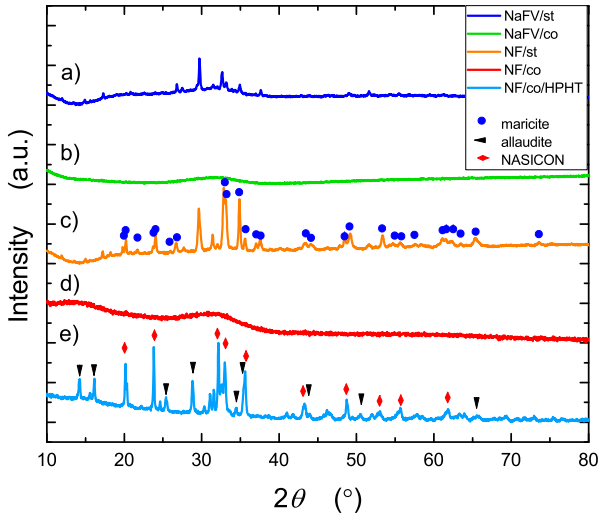

Figure 3. XRD patterns of the studied samples: a) $NaFe_{0.85}V_{0.10}PO_4$ glass quenched on steel plate (NFV/st), b) $NaFe_{0.85}V_{0.10}PO_4$ glass quenched on copper plate (NFV/co), c) $NaFePO_4$ sample quenched on steel (NF/st), d) $NaFePO_4$ glass quenched on copper (NF/co), e) $NaFePO_4$ glass after high pressure – high temperature treatment (NF/co/HPHT).Bragg peaks in patterns c) and e) correspond to identified crystalline phases (see text).

The diffractogram of NF/st sample (curve c in Figure 3) shows peaks associated mainly with $NaFePO_4$ of maricite structure, which exhibits the same composition that olivine, but its electrochemical properties are modest. In opposite to olivine (orthorhombic system), maricite exhibits a tetragonal structure. The difference between maricite and phospho-olivine is swapped locations of alkali metal (sodium or lithium) and iron between those structures. While olivine exhibits tunnels of alkali metal ions, maricite lacks those channels. This explains the difference in ionic conductivity of those two polymorphs and the difference in ability to Na^+ intercalation/deintercalation reaction.

On the other hand, a diffractogram of the sample after HPHT treatment (curve e in Figure 3) indicates a presence of electrochemically active phases like: $Na_3Fe_2(PO_4)_3$ (NASICON structure) and $Na_2Fe_3(PO_4)_3$ (alluaudite structure).

Alluaudite structure is monoclinic (space group I2/b). In this structure easy conduction pathways for sodium ions can be observed, which explains better electrochemical ability of alluaudite compared with maricite. The second identified phase - NASICON - exhibits a rhombohedral structure (space group R-3c). In this structure, similarly to alluaudite, sodium ion channels facilitating ion mobility exist.

The difference between sodium to iron ratios in alluaudite (2:3) and NASICON (3:2) phases could explain their coexistence in approximately 1:1 ratio (more precisely 9:11) in the final composites (in substrates of reaction, a ratio of sodium to iron ratio was 1:1).

Preprints (www.preprints.org) | NOT PEER-REVIEWED | Posted: 15 December 2022 doi:10.20944/preprints202212.0267.v1

Using a software associated with used diffractometer it was possible to estimate (based on Scherrer formula) average size of grains detected in the identified crystalline phases (Table 2). Nanomaterials obtained after HPHT treatment are composed of crystallites of average sizes of 91 nm (NASICON) and 42 nm (alluaudite).

Table 2. Contents of crystalline phases detected in studied samples

Phase / Structure (Ref. code)	NF/st (Crystallite size [nm])	NF/co (Crystallite size [nm])	NF/co/HPHT (Crystallite size [nm])
$Na_3Fe_2(PO_4)_3$ / NASICON (ICCD 04-011-4360)	-	-	44.7% (91 nm)
$Na_2Fe_3(PO_4)_3$ / alluaudite (ICCD 04-009-8653)	-	-	55.3% (42 nm)
$NaFePO_4$ / maricite (ICCD 04-012-9665)	100% (39 nm)	-	-

3.3. Broadband Dielectric Spectroscopy

3.3.1. Temperature dependencies of electric conductivity

Broad band dielectric spectroscopy gives wide opportunities for dielectric and electric studies of various systems. A starting point is complex electrical permittivity $\varepsilon^* = \varepsilon'(\omega) + i\varepsilon''(\omega)$, which imaginary part is responsible for electrical conduction by formula:

$$\sigma' = \sigma_{DC} + \omega\varepsilon_0\varepsilon''(\omega) \quad (1)$$

In this section we concentrate on dc conductivity determined from the real part of complex conductivity spectra. Figure 4 shows temperature dependencies of conductivity for studied samples before and after high pressure-high temperature treatment (HPHT). Results could be compared with our earlier findings concerning $LiFe_{0.75}V_{0.10}PO_4$ olivine-like cathode materials [18]. As it was already mentioned, cathode materials should exhibit mixed electronic-ionic conductivity with distinct predominance of electronic component. In fact, conductivity runs presented in Figure 4 relate to total electric conductivity, but ionic component is practically fully masked by strongly dominant and much more frequent electronic hopping between Fe^{2+} - Fe^{3+} redox couples s via oxygen bridge[11].

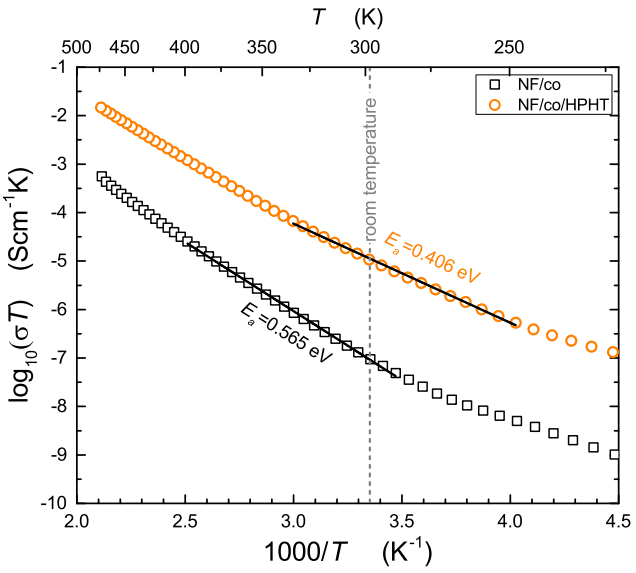

Figure 4. Temperature dependencies of electric conductivity for: $NaFePO_4$ glass quenched (NF/co) and corresponding nanocomposite after HPHT treatment (NF/HPHT).

 doi:10.20944/preprints202212.0267.v1

All experimental dependencies shown in Figure 4 can be described by well-known Mott's formulas referring to electron transport in glasses and disordered systems [13,14]. Formulas given below are valid for two different temperature ranges, characterized by Debye temperature θ_D, known from the theory of heat capacity.

For $T > \frac{\theta_D}{2}$ electron *hops are phonon assisted* (the jumps are facilitated by vibration modes) and temperature dependence of electronic conductivity is given by following Arrhenius-like expression.

$$\sigma(T)T = \nu_{el}c(1-c)\frac{e^2}{Rk_B}\exp(-2\alpha R)\exp\left(-\frac{E_a}{k_BT}\right) \quad (2)$$

where R is the average distance between hopping centers (Fe^{2+}/Fe^{3+}), k_B is Boltzmann constant, T is temperature, $\nu_{el} = \frac{h}{m_eR^2}$, α is the inverse of localization length of the electron wave function, c is the fraction of occupied hopping sites for electrons and E_a is the activation energy [13,14]. This kind of electronic transport is usually referred as hopping of small polarons, because jumps of localized electron in ionic structure is coupled with simultaneous motion of elastic deformation of local (small) surrounding [11].

For temperatures as low as $T < \frac{\theta_D}{4}$, when phonons are "frozen", and the electron transport mechanism changes to the *variable range hopping*, which follows the famous "$T^{\frac{-1}{4}}$" formula. In this temperature regime jumping electrons are looking for states of similar energies, which not necessarily correspond to adjacent, sites. The experimental dependencies of conductivity (for glass and glass-ceramics) deviate at low temperatures from the Arrhenius behavior and follow formula:

$$\sigma(T) = A\exp\left(-BT^{\frac{-1}{4}}\right) \quad (3)$$

where A and B are defined in [13,14]. Two aforementioned temperature ranges of Mott's theory are visible in Figure 4. This kind of behavior we also observed in our earlier papers [11,20]. One can see from Figure 4 that HPHT treatment considerable enhances electric conductivity (about 2 orders of magnitude) from $3.18 \cdot 10^{-10}$ S/cm to $3.58 \cdot 10^{-8}$ S/cm at room temperature (and from $2.05 \cdot 10^{-8}$ S/cm to $1.17 \cdot 10^{-7}$ S/cm at 100°C)) and decreases value of activation energy by 28%. Additionally it is worthy to note that increase in conductivity for Na composites is higher than for their Li analogues [18]. For comparison, room temperature conductivities of NASICON and tri-iron alluaudite are equal to $1.33 \cdot 10^{-10}$ S/cm[15] and $8.78 \cdot 10^{-12}$ S/cm[21] respectively.

3.3.2. Temperature dependencies of relaxation times

Electric conduction is a macroscopic phenomenon and measurement of dc conductivity may not provide microscopic insight into occurring process. Separation of component processes, contributing to total conductivity and dielectric response is possible thanks to various spectroscopic representations. In this study we used analysis of electric modulus interrelated with complex electrical permittivity by formula.

$$M^* = \frac{1}{\varepsilon^*(\omega)} = M'(\omega) + iM''(\omega) = \frac{\varepsilon'(\omega)}{\varepsilon'^2(\omega)+\varepsilon''^2(\omega)} + i\frac{\varepsilon''(\omega)}{\varepsilon'^2(\omega)+\varepsilon''^2(\omega)} \quad (4)$$

Imaginary part of electric modulus $M''(\omega) = \frac{\varepsilon''(\omega)}{\varepsilon'^2(\omega)+\varepsilon''^2(\omega)}$ gives information of relaxation processes related to transport of various charge carriers in studied materials.

Preprints (www.preprints.org) | NOT PEER-REVIEWED | Posted: 15 December 2022 doi:10.20944/preprints202212.0267.v1

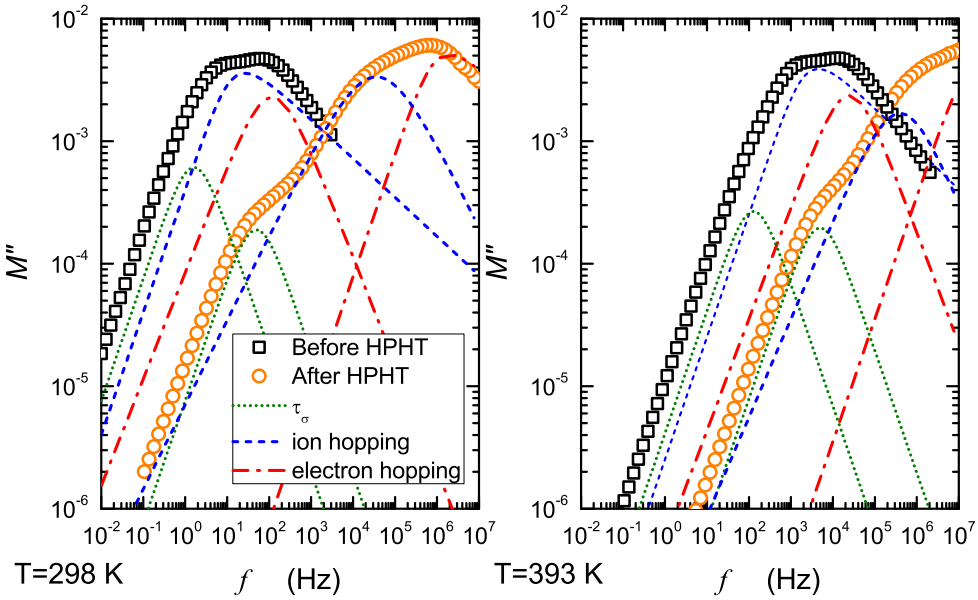

Figure 5. Resolved spectra of imaginary part of electric modulus for studies samples before and after HPHT treatment at 298 K and 393 K.

Figures 5 and 6 present deconvoluted spectra of imaginary parts of electric modulus. Straight parts correspond to dc-conductivity, whereas peaks apparently relate to relaxation times: of ion hopping (τ_{ih}), electron hopping (τ_{eh}) and ion motion (τ_{σ}) through grain boundaries induced by HPHT.Almost invisible effect, resembling inter cluster transport, corresponding probably to small heterogeneity was also observed in starting glasses. It was taken into consideration to improve fit of the spectra before HPHT. Different mechanisms of ion transfer in solids are broadly discussed in [22–25]. Transport of ions and electrons related with dc-conductivity describes long range properties of material. On the other hand, hopping (which is also contributes to dc conduction) is mainly related to ac-conductivity and might be described by temperature activated processes.

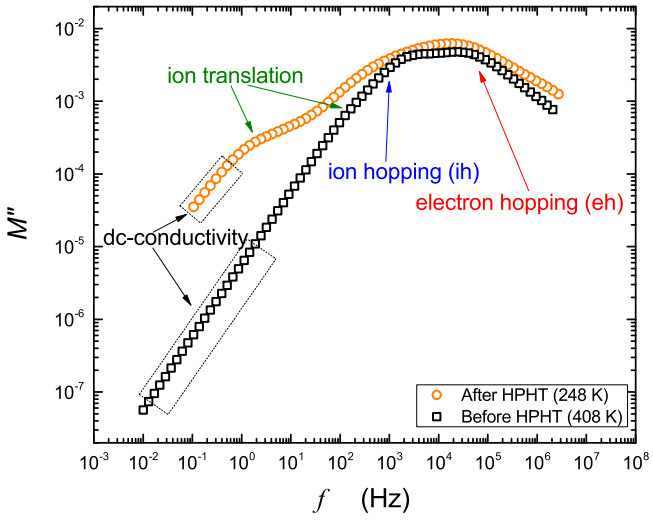

Figure 6. Temperature-time-scaling (TTS) for studied samples before and after HPHT treatment. Inter-grain ion transport, intra-grain ion hopping (ih) and electron hopping (eh) are resolved. Note that curves correspond to 248 and 408 K, what gives 160 K shift

Preprints (www.preprints.org) | NOT PEER-REVIEWED | Posted: 15 December 2022 doi:10.20944/preprints202212.0267.v1

Taking into consideration common properties of cathode materials one can postulate that low frequency processes resolved from spectra in Figure 5 correspond to ionic conduction and high frequency ones refer to electronic conduction. In fact, ionic conductivity in studied materials is very low (jumps of Na^+ are slow) and electronic conduction predominates, because hopping of electrons is much more frequent. Further conclusions resulting from Figure 5 are as follows: *i*) HTHP treatment leads to considerable shift of modulus peaks towards much higher frequencies, *ii*) appearance of low frequency arm is correlated with pressure induced crystallization of studied samples.

Resolved spectra of allowed to determine relaxation times corresponding to related processes. According to widely accepted Havriliak-Negami relation [26,27] it was assumed following relationship between frequency (f_{max}) of maximum of and relaxation time τ:

$$\omega_{max} = \tau^{-1}\left(\frac{\sin(\frac{\alpha\pi}{2(\beta+1)})}{\sin(\frac{\alpha\beta\pi}{2(\beta+1)})}\right)^{1/\alpha} \quad (5)$$

where α and β are parameters of H-N relaxation element. Taking into account a frequency range (and values of H-N parameters) in our measurements it was possible to approximate this formula into a simpler form $\tau = (2\pi f_{max})^{-1}$.

The calculated values of relaxation time τ plotted in Arrhenius temperature scale are given in Figure 7. Pressure induced reduction of relaxation times is observed in the whole temperature range. Before HPHT treatment, electron as well as ionic hopping are thermally activated exhibiting single activation energy. After HPHT, temperature dependencies of relaxation times become non-Arrhenius in some ranges, apparently due to heterogeneity caused by crystallization of 2 new phases. This is clearly visible for relaxation process related to inter-grain transport of ions (green curve in Figure 7).

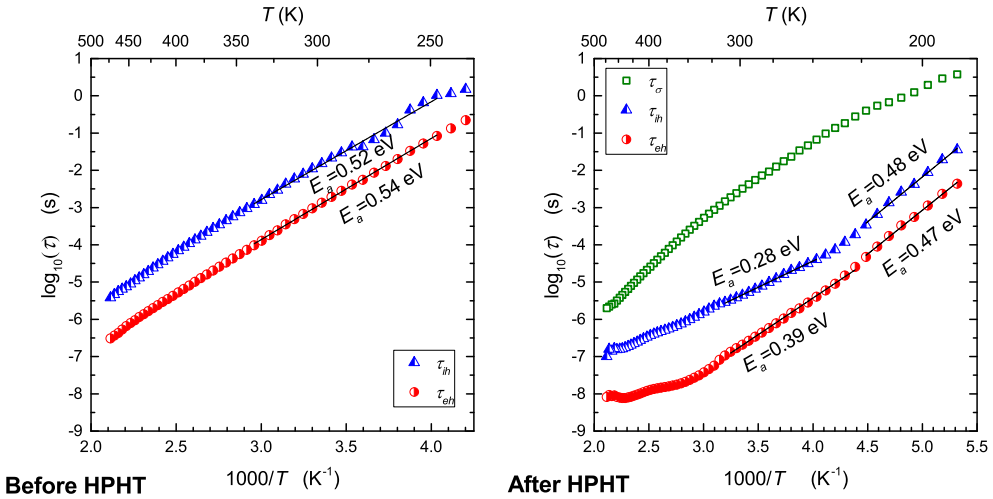

Figure 7. Temperature dependencies of relaxation time for various processes revealed in measurements of electric modulus, before and after HPHT treatment.

Comparing Figures 4 and 7 and taking into account only electron hopping, it is visible that the corresponding values of activation energies determined from temperature dependencies of relaxation time (0.54 eV, 0.39 eV) and electric conductivity (0.54 eV, 0,40 eV) are the same within limits of experimental uncertainty. It is also seen that HPHT treatment disturbs Arrhenius behavior for temperature higher than 350 K and changes mechanism of transport for temperature lower than 220 K (Figure 7).

4. Discussion

Hopping of electrons required adjacent Fe^{2+}/Fe^{3+} centers. On the other hand hopping of ions requires empty sites in the vicinity of given Na^+ cation. After HPHT treatment a

 doi:10.20944/preprints202212.0267.v1

ramified network of grain boundaries appear. Defective surfaces of those boundaries are a source of aliovalent iron centers. Therefore in such conditions transport of electrons occurs mainly along grain boundaries (highly disordered nanocrystallite shells) and transport of ions occurs across grain boundaries (inter-grain) and in bulk of crystallites (intra-grain). Taking into account experimental data obtained in this work and general properties of cathode materials one can conclude that hopping of electrons is the fastest process of charge transport occurring in studied samples. Consequently, electric conduction is dominated by electronic component of total conductivity and ionic component is strongly suppressed. It seems that, enhancement of electronic conductivity after HPHT treatment (Figure 4) has quite natural and intuitive interpretation. It can be seen from formula (3) that electronic conductivity depends (like $\frac{1}{R}$) on average distance between hopping centers (Fe^{2+}- Fe^{3+}). Similarly, activation energy E_a of electron hopping decreases when R shortens, because E_a =const.$\cdot(1-\frac{r_p}{R})$, where r_p denotes a radius of small polaron [14]. This is consistent with expected reduction of distances between atoms after high pressure treatment. In disordered systems containing iron, electron hopping occurs via oxygen bridge, between Fe^{2+} and Fe^{3+} centers[11]. The concentration of such aliovalent ions in nanomaterials is much higher than in glasses and polycrystalline materials and therefore hopping is much more effective in such systems. This is effect of large surface to grain volume ratio in nanomaterials. An external high pressure additionally increases this effect because of reduction of distance between Fe^{2+}/Fe^{3+} redox couples. Observed reduction of relaxation times (Figure 7) occurs because of the same mechanism. It is seen, from comparison of Figures 4 and 7, that values of activation energies determined from electronic conductivity and relaxation time measurements are almost the same. Effect of high pressure is also observed in the case of Na^+ jumps. Relaxation time as well and corresponding activation energy considerably change after HPHT treatment (τ decreased by one order of magnitude and E_a decreased from 0.52 to 0.28 eV in the middle range of temperature, cf. Figure 7). As a result of high pressure – high temperature treatment initial glass transformed into two-phase nanocomposite - consequently grain boundaries appeared in studied sample. This caused a non-Arrhenius behavior of the process related to inter-grain transport (green plot in Figure 7). Additionally, intra-grain (bulk) ionic motion exhibits 2 activation energies apparently due to 2 nanocrystalline phases induced by HPHT treatment.

5. Conclusions

A new preparation method of cathode materials for sodium batteries was proposed by using high pressure – high temperature treatment of initial glass of composition $NaFePO_4$. Applying a pressure of 1 GPa effectively enhanced electrical conductivity of studied material and induced two electrochemically active phases – NASICON and alluaudite. It was shown that effect of high pressure has been permanent and lasted for several months. Other advantage of high-pressure cathode materials is their anticipated higher volumetric capacity compared with standard cathodes with carbon additions. It was demonstrated that combination of high pressures and broadband dielectric spectroscopy is a powerful method to resolve various relaxation processes and molecular movements in solids. Particularly, in this study it was possible to separate electronic and ionic components of electric charge movement.

Author Contributions: Sample preparation, data acquisition and analysis, measurements, writing, sharing ideas, A. Sz-Sz.; Data analysis, writing, discussions, sharing ideas, S. S.; Sample preparation, writing- discussion, T. K. P.; Conceptualization, writing, discussions, supervision, sharing ideas, interpretation, J.E.G.; Conceptualization, discussions, S.J.R.; Consulting, discussions, M.B.; All authors have read and agreed to the published version of the manuscript.

Funding: This research received no external funding.

Data Availability Statement: Data is available from authors on reasonable request.

Conflicts of Interest: The authors declare no conflict of interest.

References

1. Meins, J.L.; Crosnier-Lopez, M.; Hemon-Ribaud, A.; Courbion, G. Phase Transitions in the $Na_3M_2(PO_4)_2F_3$ Family (M =Al^{3+}, V^{3+}, Cr^{3+}, Fe^{3+}, Ga^{3+}): Synthesis, Thermal, Structural, and Magnetic Studies. *Journal of Solid State Chemistry* **1999**, *148*, 260 – 277. https://doi.org/10.1006/jssc.1999.8447.
2. Shakoor, R.A.; Seo, D.H.; Kim, H.; Park, Y.U.; Kim, J.; Kim, S.W.; Gwon, H.; Lee, S.; Kang, K. A combined first principles and experimental study on $Na_3V_2(PO_4)_2F_3$ for rechargeable Na batteries. *J. Mater. Chem.* **2012**, *22*, 20535–20541. https://doi.org/10.1039/C2JM33862A.
3. Matts, I.L.; Dacek, S.; Pietrzak, T.K.; Malik, R.; Ceder, G. Explaining Performance-Limiting Mechanisms in Fluorophosphate Na-Ion Battery Cathodes through Inactive Transition-Metal Mixing and First-Principles Mobility Calculations. *Chemistry of Materials* **2015**, *27*, 6008–6015. https://doi.org/10.1021/acs.chemmater.5b02299.
4. Trad, K.; Carlier, D.; Croguennec, L.; Wattiaux, A.; Amara, M.B.; Delmas, C. $NaMnFe_2(PO_4)_3$ Alluaudite Phase: Synthesis, Structure, and Electrochemical Properties As Positive Electrode in Lithium and Sodium Batteries. *Chemistry of Materials* **2010**, *22*, 5554–5562. https://doi.org/10.1021/CM1015614.
5. Dwibedi, D.; Barpanda, P.; Yamada, A. Alluaudite Battery Cathodes. *Small Methods* **2020**, *4*, 2000051. https://doi.org/10.1002/smtd.202000051.
6. Padhi, A.K.; Nanjundaswamy, K.S.; Goodenough, J.B. Phospho-olivines as Positive-Electrode Materials for Rechargeable Lithium Batteries. *Journal of The Electrochemical Society* **1997**, *144*, 1188–1194. https://doi.org/10.1149/1.1837571.
7. Fang, Y.; Zhang, J.; Xiao, L.; Ai, X.; Cao, Y.; Yang, H. Phosphate Framework Electrode Materials for Sodium Ion Batteries. *Advanced Science* **2017**, *4*, 1600392. https://doi.org/10.1002/advs.201600392.
8. Zaghib, K.; Trottier, J.; Hovington, P.; Brochu, F.; Guerfi, A.; Mauger, A.; Julien, C. Characterization of Na-based phosphate as electrode materials for electrochemical cells. *Journal of Power Sources* **2011**, *196*, 9612–9617. https://doi.org/10.1016/j.jpowsour.2011.06.061.
9. Kim, J.; Seo, D.H.; Kim, H.; Park, I.; Yoo, J.K.; Jung, S.K.; Park, Y.U.; Goddard, W.; Kang, K. Unexpected discovery of low-cost maricite $NaFePO_4$ as a high-performance electrode for Na-ion batteries. *Energy Environ. Sci.* **2015**, *8*, 540–545. https://doi.org/10.1039/C4EE03215B.
10. Bong, J.H.; Adams, S. Molecular dynamics simulations of amorphous $NaFePO_4$ as an Na-ion battery cathode material. *Functional Materials Letters* **2021**, *14*, 2141006. https://doi.org/10.1142/S179360472141006X.
11. Pietrzak, T.K.; Wasiucionek, M.; Garbarczyk, J.E. Towards Higher Electric Conductivity and Wider Phase Stability Range via Nanostructured Glass-Ceramics Processing. *Nanomaterials* **2021**, *11*. https://doi.org/10.3390/nano11051321.
12. Garbarczyk, J.E.; Pietrzak, T.K.; Wasiucionek, M.; Kaleta, A.; Dorau, A.; Nowiński, J.L. High electronic conductivity in nanostructured materials based on lithium-iron-vanadate-phosphate glasses. *Solid State Ionics* **2015**, *272*, 53–59. https://doi.org/10.1016/j.ssi.2014.12.019.
13. Mott, N. Electrons in disordered structures. *Advances in Physics* **1967**, *16*, 49–144. https://doi.org/10.1080/00018736700101265.
14. Austin, I.; Mott, N. Polarons in crystalline and non-crystalline materials. *Advances in Physics* **1969**, *18*, 41–102. https://doi.org/10.1080/00018736900101267.
15. Pietrzak, T.K.; Kruk-Fura, P.E.; Mikołajczuk, P.J.; Garbarczyk, J.E. Syntheses and nanocrystallization of $NaF–M_2O_3–P_2O_5$ NASICON-like phosphate glasses (M = V, Ti, Fe). *International Journal of Applied Glass Science* **2020**, *11*, 87–96. https://doi.org/10.1111/ijag.13643.
16. Nowagiel, M.; Samsel, M.J.; Pietrzak, T.K. Towards the High Phase Purity of Nanostructured Alluaudite-Type Glass-Ceramics Cathode Materials for Sodium Ion Batteries. *Materials* **2021**, *14*. https://doi.org/10.3390/ma14174997.
17. Nowagiel, M.; Samsel, M.J.; Kazakevicius, E.; Zalewska, A.; Kežionis, A.; Pietrzak, T.K. Electrochemical Performance of Highly Conductive Nanocrystallized Glassy Alluaudite-Type Cathode Materials for NIBs. *Energies* **2022**, *15*. https://doi.org/10.3390/en15072567.
18. Baranowski, P.; Starzonek, S.; Drozd-Rzoska, A.; Rzoska, S.J.; Bockowski, M.; Keblinski, P.; Pietrzak, T.K.; Garbarczyk, J.E. Multifold pressure-induced increase of electric conductivity in $LiFe_{0.75}V_{0.10}PO_4$ glass. *Scientific Reports* **2019**. https://doi.org/10.1038/s41598-019-53232-z.
19. Smedskjaer, M.M.; Bauchy, M.; Mauro, J.C.; Rzoska, S.J.; Bockowski, M. Unique effects of thermal and pressure histories on glass hardness: Structural and topological origin. *The Journal of Chemical Physics* **2015**, *143*, 164505. https://doi.org/10.1063/1.4934540.
20. Pietrzak, T.; Garbarczyk, J.; Gorzkowska, I.; Wasiucionek, M.; Nowinski, J.; Gierlotka, S.; Jozwiak, P. Correlation between electrical properties and microstructure of nanocrystallized $V_2O_5–P_2O_5$ glasses. *Journal of Power Sources* **2009**, *194*, 73–80. XIth Polish Conference on Fast Ionic Conductors 2008, https://doi.org/10.1016/j.jpowsour.2009.02.031.
21. Chamryga, A.E.; Nowagiel, M.; Pietrzak, T.K. Syntheses and nanocrystallization of $Na_2O–M_2O_3–P_2O_5$ alluaudite-like phosphate glasses (M = V, Fe, Mn). *Journal of Non-Crystalline Solids* **2019**, *526*, 119721. https://doi.org/10.1016/j.jnoncrysol.2019.119721.
22. Almond, D.; Duncan, G.; West, A. The determination of hopping rates and carrier concentrations in ionic conductors by a new analysis of ac conductivity. *Solid State Ionics* **1983**, *8*, 159–164. https://doi.org/10.1016/0167-2738(83)90079-6.
23. Almond, D.; Hunter, C.; West, A. The Extraction of Ionic Conductivities and Hopping Rates from ac Conductivity Data. *Journal of Materials Science* **1984**, *19*, 3236–3248. https://doi.org/10.1007/BF00549810.
24. Dyre, J.C.; Schrøder, T.B. Hopping models for ion conduction in noncrystals. In *Superionic Conductor Physics*; World Scientific, 2007; pp. 97–102.

 doi:10.20944/preprints202212.0267.v1

25. Morgan, B.J. Understanding fast-ion conduction in solid electrolytes. *Philosophical Transactions of the Royal Society A: Mathematical, Physical and Engineering Sciences* **2021**, *379*, 20190451. https://doi.org/10.1098/rsta.2019.0451.
26. Chełkowski, A. *Fizyka dielektryków*; Wydawnictwo Naukowe PWN: Warszawa, 1993.
27. Jonscher, A.K. *Dielectric relaxation in solids*; Chelsea Dielectrics Press: London, 1983.